

Energetic decomposition yields efficient bimetallic Cu MOF-derived catalysts Supplementary Information

Anh H. T. Nguyen Sorenson^a, Yu Wu^c, Emma K. Orcutt^a, Rosalyn V. Kent^b, Hans C. Anderson^a, Adam J. Matzger^b and Kara J. Stowers^{a*}

^a Department of Chemistry and Biochemistry Department, Brigham Young University, Provo, Utah, 84604, USA.

^b Department of Chemistry and Macromolecular Science and Engineering Program, University of Michigan, 930 North University Ave, Ann Arbor, Michigan 48109-1055, USA.

^c College of Chemistry and Environmental Engineering, Sichuan University of Science & Engineering, Zigong, 643000, P. R. China
Author email: kstowers@chem.byu.edu

Table of Contents

1. Experimental Procedures and Methods
2. Powder X-Ray (PXRD) Analysis
3. Raman Spectroscopy Analysis
4. N₂ Sorption Isotherms
5. X-Ray Photoelectron Spectroscopy (XPS) Analysis
6. Scanning Transmission Electron Microscopy-Energy Dispersive X-ray Spectroscopy
7. Reduction of 4-Nitrophenol Obtained from UV-Vis
8. Reduction of 4-Nitro-aromatic Compounds from UV-Vis
9. References

1. Experimental procedures and methods

Synthesis and activation of HKUST-1

Synthesis of HKUST-1 was performed according to previous literature reported methods.¹ The as-synthesized HKUST-1 was immersed in CH_2Cl_2 for 24 h, exchanging with fresh CH_2Cl_2 every 8 h, and then activated under dynamic vacuum at a constant temperature of 120 °C for 24 h. After activation, the as-synthesized HKUST-1 was stored in a nitrogen filled glove box.

Synthesis of HKUST-1/TNT (CuO@C) and thermolysis procedure

25 mg of activated HKUST-1 crystals and 50 mg of TNT were added to a 4 mL vial in the glove box and shaken for 5 minutes. The vial was removed from the glovebox and then heated at 90 °C for 2 h. The explosive mixture was then carefully transferred to a copper pan and sealed. The pan was placed inside of a quartz tube with one end sealed and the other open to air. A special lip was melted into the side of the tube where the pan rests prior to initiation. A torch was then used to pre-heat the sealed end. Once heated for a few seconds, the copper pan was knocked into the hot region and thermally initiated. CuO/C was captured in an Erlenmeyer flask at the open end of the tube and collected for analysis.

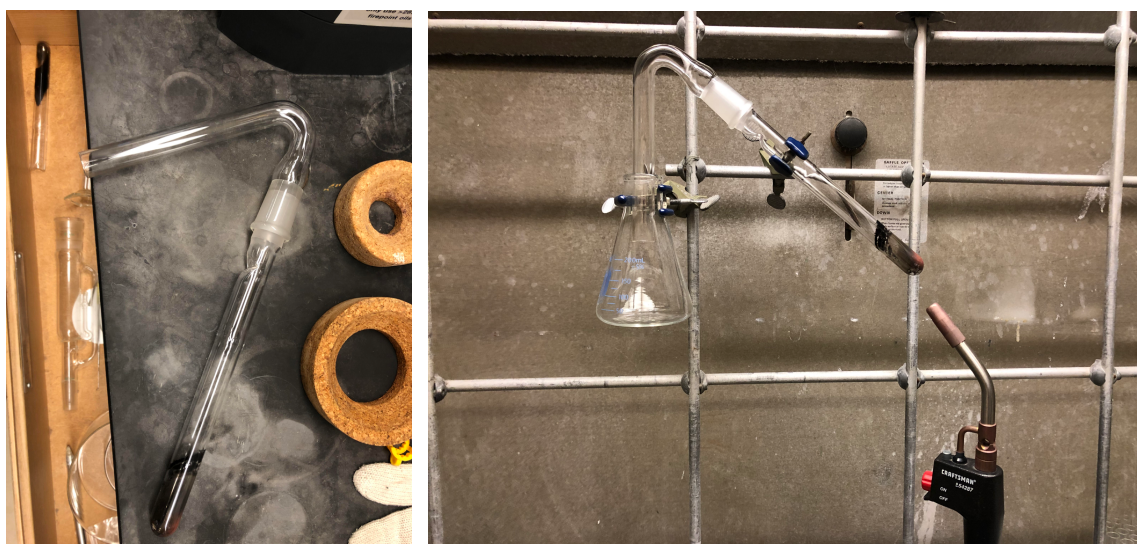


Figure S1. a) Left: Quartz tube designed to hold copper pan on a small lip near joint prior to thermolysis b) Right: Thermolysis setup with quartz tube and butane torch used to heat samples. Upon degradation the material was collected in an Erlenmeyer flask.

Synthesis of HKUST-1/TNT/Ag (Ag-CuO@C)

800 mg of activated HKUST-1 crystals and 17 mg of AgNO_3 were added to a 20 mL glass vial in a nitrogen filled glovebox. The vial was shaken by hand for 5 minutes. The vial was removed from the glovebox and 1.5 mL of methanol was added to the mixture. This vial was shaken by hand again for 5 minutes. Finally, the suspension was placed in a shaker at room temperature for 7 days. To avoid destroying the crystal structure of HKUST-1, we chose to shake the mixture samples, which is a comparatively mild method but takes a slightly longer time compared to vigorous stirring. We did not optimize the timing of the process and this likely could be carried out faster. As HKUST-1 was immersed in the solution of metal salts therefore, when methanol evaporates, the dissolved metal salts doped on the inside channels or outside surface of HKUST-1. However, the long shaking time ensures plenty of time for diffusion into the pores of the MOF and the slow evaporation of the methanol ensures continuous saturation of the TNT solution as the TNT is adsorbed into the pores. Methanol was then evaporated by a slow stream of air flowing over the

uncapped vial for 2h. The solid $\text{AgNO}_3/\text{HKUST-1}$ composite was collected. 25 mg of $\text{AgNO}_3/\text{HKUST-1}$ and 50 mg of TNT were added to a 4 mL vial in the glove box and shaken by hand for 5 minutes. The vial was removed from the glovebox and then heated at 90 °C for 2 h. The explosive mixture was then carefully transferred to a copper pan and sealed. The copper pans are 10 mm diameter and 5 mm deep composed of one copper pan and one copper lid. The material is added and then a slightly narrower lid is pressed in to compress the material and ensure good thermal contact. The copper pan and lid were sealed by carefully pushing them together using a tweezer. As for yield, no attempt was made to quantify the maximum yield, which would require collecting the deflagration products from the entire thermolysis tube. The average yield of product collected is about 25%. Finally, $\text{Ag}/\text{CuO}/\text{C}$ was produced by the thermolysis procedure detailed above.

Synthesis of HKUST-1/TNT/Ni (Ni-CuO@C)

800 mg of activated HKUST-1 crystals and 53 mg of $\text{Ni}(\text{NO}_3)_2 \cdot 6\text{H}_2\text{O}$ were added to a 20 mL glass vial in a nitrogen filled glovebox. The vial was shaken by hand for 5 minutes. The vial was removed from the glovebox and 1.5 mL of methanol was added to the mixture. This vial was shaken by hand again for 5 minutes. Finally, the suspension was placed in a shaker at room temperature for 7 days as described in the Ag-CuO@C procedure. Methanol was then evaporated by a slow stream of air flowing over the uncapped vial for 2h. The solid $\text{Ni}(\text{NO}_3)_2/\text{HKUST-1}$ composite was collected. 25 mg of $\text{Ni}(\text{NO}_3)_2/\text{HKUST-1}$ and 50 mg of TNT were added to a 4 mL vial in the glove box and shaken by hand for 5 minutes. The vial was removed from the glovebox and then heated at 90 °C for 2 h. The explosive mixture was then carefully transferred to a copper pan and sealed. Finally, $\text{Ni}/\text{CuO}/\text{C}$ was produced by the thermolysis procedure detailed above.

Synthesis of HKUST-1/TNT/Co (Co-CuO@C)

800 mg of activated HKUST-1 crystals and 53 mg of $\text{Co}(\text{NO}_3)_2 \cdot 6\text{H}_2\text{O}$ were added to a 20 mL glass vial in a nitrogen filled glovebox. The vial was shaken by hand for 5 minutes. The vial was removed from the glovebox and 1.5 mL of methanol was added to the mixture. This vial was shaken by hand again for 5 minutes. Finally, the suspension was placed in a shaker at room temperature for 7 days as described in the Ag-CuO@C procedure. Methanol was then evaporated by a slow stream of air flowing over the uncapped vial for 2h. The solid $\text{Co}(\text{NO}_3)_2/\text{HKUST-1}$ composite was collected. 25 mg of $\text{Co}(\text{NO}_3)_2/\text{HKUST-1}$ and 50 mg of TNT were added to a 4 mL vial in the glove box and shaken by hand for 5 minutes. The vial was removed from the glovebox and then heated at 90 °C for 2 h. The explosive mixture was then carefully transferred to a copper pan and sealed. Finally, $\text{Co}/\text{CuO}/\text{C}$ was produced by the thermolysis procedure detailed above.

Powder X-Ray diffraction.

Powder patterns were collected with a Panalytical Empyrean using $\text{Cu-K}\alpha$ radiation ($\lambda = 1.54187 \text{ \AA}$) and operating at 45 kV and 40 mA. The instrument is equipped with a Bragg-Brentano HD X-ray optic and an X'Celerator Scientific detector operating in continuous 1D scanning mode. Samples were prepared by pressing them onto a glass slide fitted into a sample holder to minimize height error. The patterns were collected by scanning 2θ from 5° to 50° with a 0.02° step size and a step speed of 0.125 seconds. The data were processed using Jade 8 XRD Pattern Processing, Identification & Quantification analysis software (Materials Data, Inc.). The powder patterns were compared to respective simulated powder patterns from single crystal XRD structures available from the Cambridge Crystallographic Data Centre and were found to be in good agreement with the predicted patterns.

Gas sorption measurements.

Sorption experiments were carried out using a NOVA - series 4200 surface area analyzer (Quantachrome Instruments, Boynton Beach, Florida, USA). N₂ (99.999%) was purchased from Cryogenic Gases and used as received. For N₂ measurements, a glass sample cell was charged with ~50 to 100 mg of sample and analyzed at 77 K. Sorption isotherms were collected in the NOVAwin software.

Raman spectroscopy.

Raman spectra were collected using a Renishaw inVia Raman Microscope equipped with a Leica microscope, 633 nm laser, 1800 lines/mm grating, 50 μm slit and a RenCam CCD detector. Spectra were collected in extended scan mode with a range of 2500-100 cm⁻¹ and analyzed using the WiRE 3.4 software package (Renishaw). Calibration was performed using a silicon standard in static mode.

Scanning transmission electron microscopy-energy dispersive X-ray spectroscopy

Scanning transmission electron microscopy-energy dispersive X-ray spectroscopy (STEM-EDX) and TEM studies were performed on a Tecnai F20 TEM using an accelerating voltage of 200 kV.

X-ray photoelectron spectroscopy

The electronic binding energy of the sample was examined by X-ray photoelectron spectroscopy (XPS) using a Surface Science SSX-100 XPS instrument (Service Physics, Bend, OR) with a monochromatic Al Kα source (1486.7 eV) and a hemispherical analyzer. The catalyst spectrum was referenced to the main C_{1s} peak in the narrow scan, which was taken at 284.5 eV. Peak fitting was performed using instrument software ('CASA XPS'). The curve-fitting of the Cu_{2p3/2}, O_{1s}, N_{1s}, and C_{1s} lines for Cu-based catalysts was employed using Gaussian (70%)–Lorentzian (30%) peak-shapes, respectively (defined in CasaXPS as GL (30)).

Inductively coupled plasma -optical emission spectrometry

The Cu wt% loading and M (M = Ni, Co, and Ag) wt% loading were determined by inductively coupled plasma optical emission spectrometry from Perkin-Elmer Optima (8300 ICP-OES) using argon and a collision cell filled with ultra-high-purity helium both from Airgas. The plasma, auxiliary and nebulizer were set to be 12, 0.2 and 0.70 L/min, respectively. The RF power was set at 1500 Watts. The flow rate pump was set 1.5 mL/min. Syngistix software was used for the analysis.

UV-Vis

The kinetic studies were performed on an Agilent 8453 G1103A Spectrophotometer. A quartz cuvette was used to hold the sample during data collection to minimize spectral interference in the region of interest. Tungsten and deuterium lamps were used to produce visible and ultraviolet light respectively. The Agilent 845x UV-Visible System program was used to collect and export all UV-Vis spectra.

Reduction of Nitroaromatic Compounds – UV-Vis Studies

For UV-Vis studies, the reduction of nitroaromatic compounds in the presence of Cu-based catalysts was carried out according to the following procedure. In a typical experiment, 1 mg of catalyst was measured and transferred into a 100 mL beaker containing 56 mL of D.I. water and a stir bar. Under vigorous stirring, 10 mL solution of 4.0 mM 4-nitroaromatic compound was added to the beaker and 0.5 mL aliquot was withdrawn from the reaction solution and recorded as initial point of kinetic run (A₀). Then, 10 mL

solution of 0.4 M sodium borohydride was added to reaction and kinetic run was started immediately. A 0.5 mL aliquot was withdrawn from the reaction solution and diluted with 2 mL D.I. water in a quartz cuvette for UV-Vis spectra at different time interval. Spectra were collected in the range of 200-900 nm every 50 seconds until the reaction reached completion (disappearance of yellow color). The corresponding amine products were confirmed by the GC-MS. Catalyst leaching was confirmed by ICP-OES.

Reduction of Nitroaromatic Compounds – Batch Reactions

For a typical batch reaction, nitrobenzene (1 mmol) and 3 mL of THF:H₂O (1:2) solution were added into a 40 mL pressurized tube in sequence, followed by the addition of catalyst (0.01-0.05 mmol Cu loading) to the mixture. NaBH₄ (3 mmol) was dissolved in 5 mL D.I. H₂O and added dropwise to the reaction mixture under vigorous stirring. The mixture was stirred for 2 h at 70 °C. Once the reaction was completed, it was cooled to room temperature followed by a filtration. The filtrate was washed with CH₂Cl₂. The organic layer was washed with brine solution and D.I. H₂O. Then, it was dried with anhydrous Na₂SO₄ and filtered. The solvent was removed under vacuum. A yield of aniline product was determined by integration using an internal standard biphenyl in the GC-MS. Catalyst leaching was confirmed by ICP-OES.

2. Powder X-Ray (PXRD) Analysis

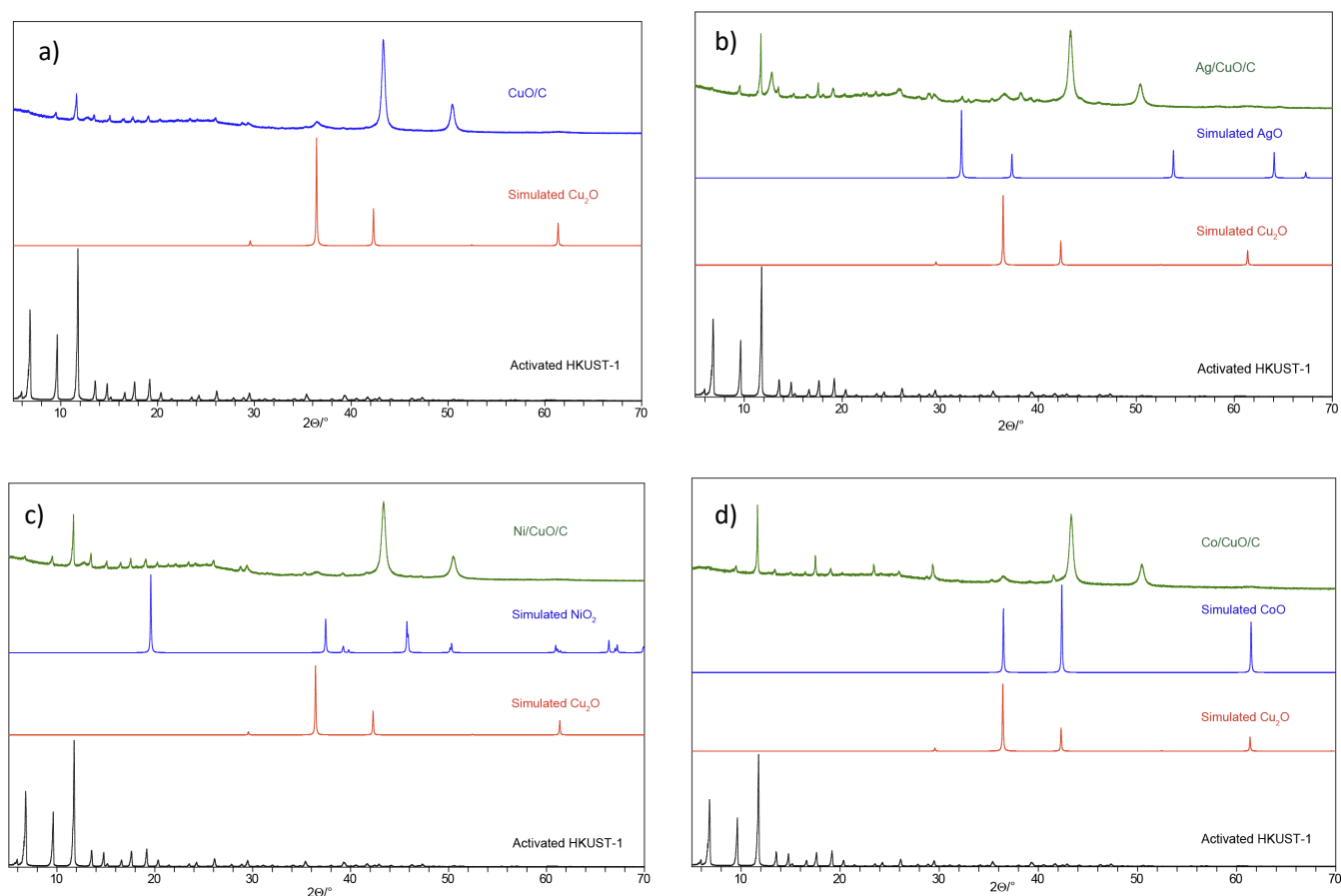


Figure S2. HKUST-1/TNT Powder X-Ray diffraction pattern a) CuO@C, b) Ag-CuO@C, c) Ni-CuO@C, d) Co-CuO@C

Table S1. The average crystallite sizes obtained from PXRD.

Catalyst	ICDD References Used	Copper	Particle Size (nm)
CuO@C	00-004-0836 (NS)	Cu(0)	18.5
	00-007-9767 (NS)	Cu(I)	11.3 ± 3.3
Ni-CuO@C	00-004-0836 (NS)	Cu(0)	13.4
	00-005-0667 (NS)	Cu(I)	6.8 ± 1.8
Co-CuO@C	01-071-4610 (NS)	Cu(0)	13.8
	01-078-2076 (NS)	Cu(I)	13.9 ± 2.8
Ag-CuO@C	00-004-0836 (NS)	Cu(0)	13.3

4. N₂ sorption isotherms

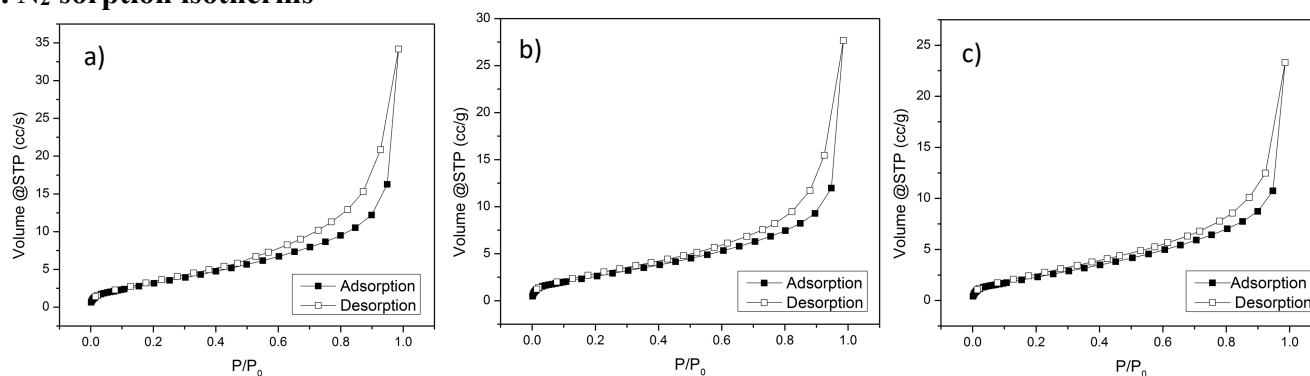


Figure S3. Nitrogen sorption isotherm collected on HKUST-1/TNT/M, a) Ag-CuO@C, b) Co-CuO@C, c) Ni-CuO@C.

5. X-Ray Photoelectron Spectroscopy Analysis

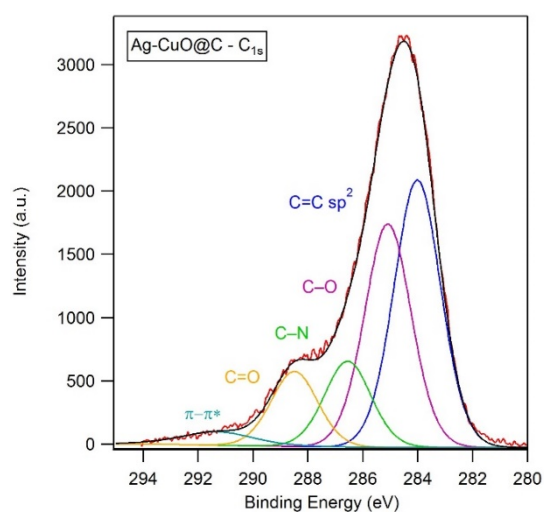
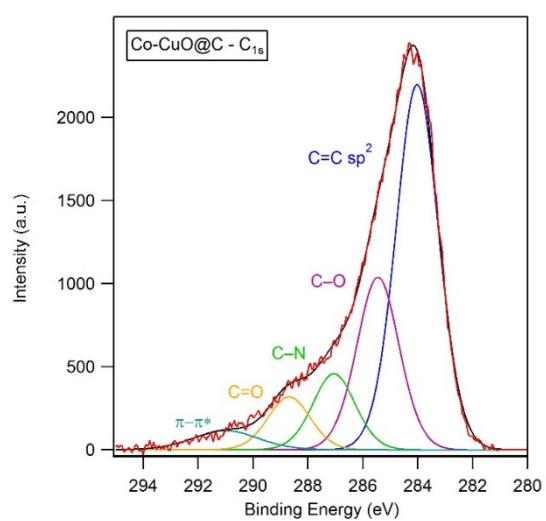
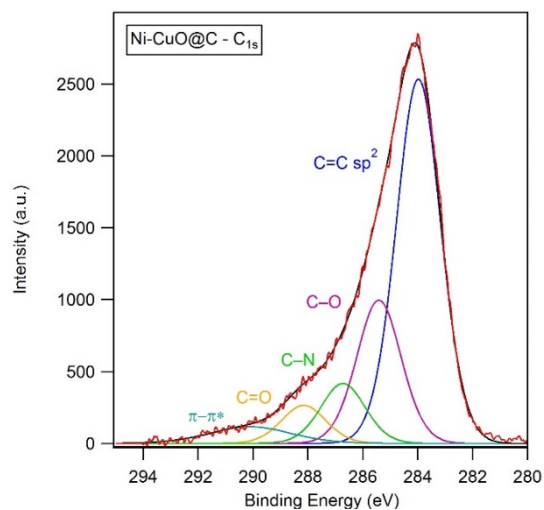
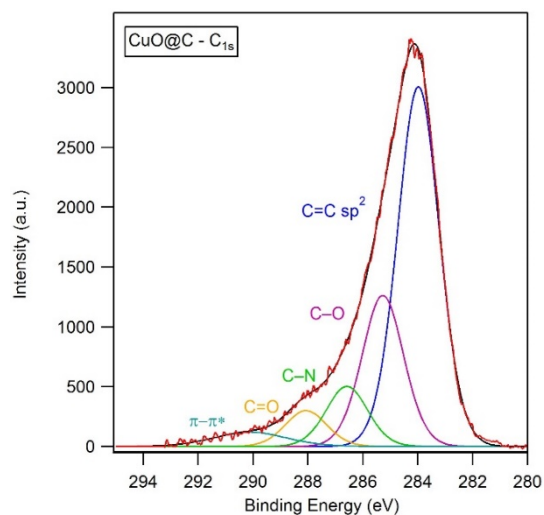


Figure S4. XPS – C_{1s} peaks for CuO@C and M-CuO@C.

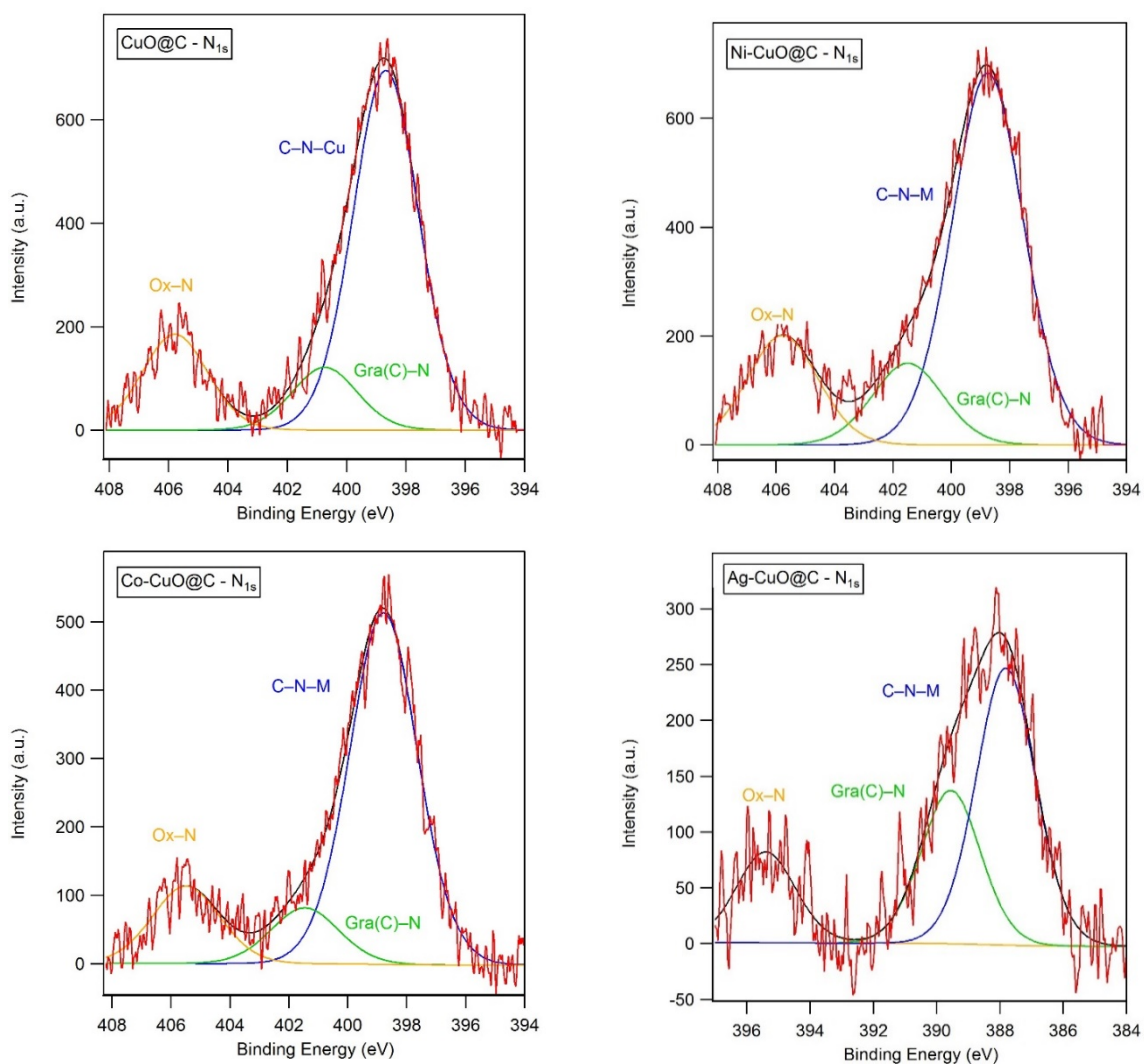


Figure S5. XPS – N_{1s} peaks for CuO@C and M-CuO@C.

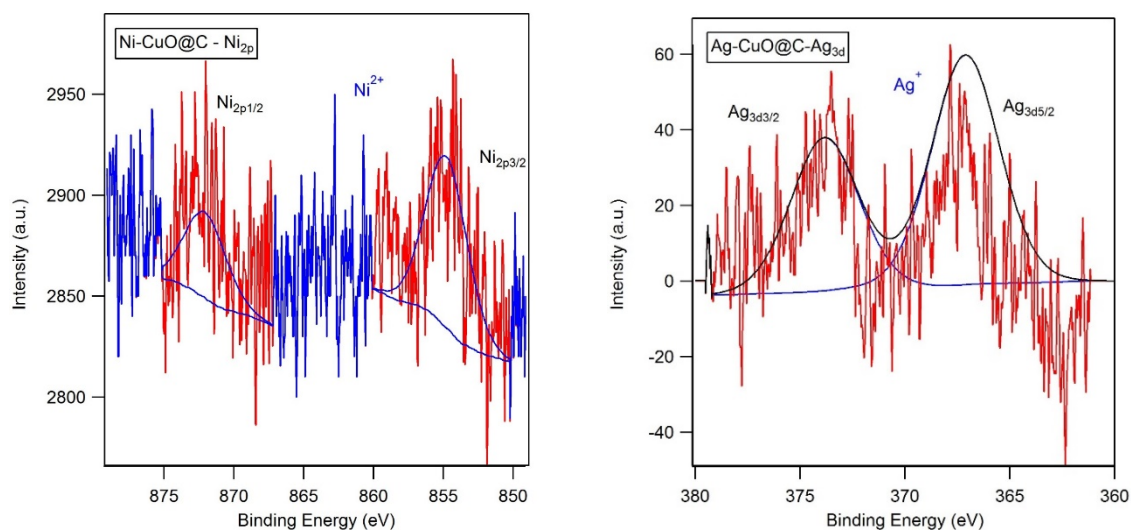


Figure S6. XPS – Ni_{2p} and Ag_{3d} peaks for Ni-CuO@C and Ag-CuO@C.

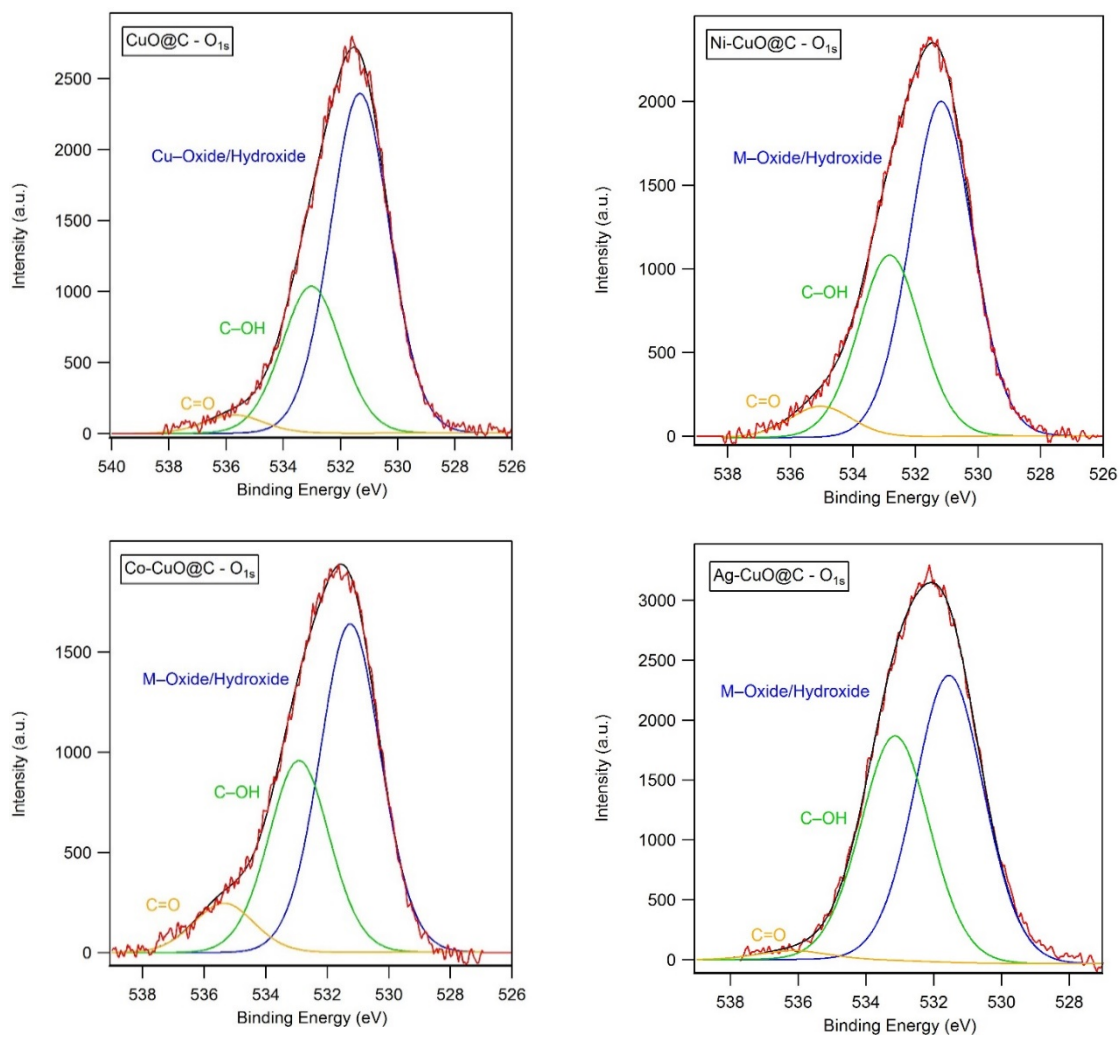


Figure S7. XPS – O_{1s} peaks for CuO@C and M-CuO@C.

3. Raman Spectroscopy Analysis

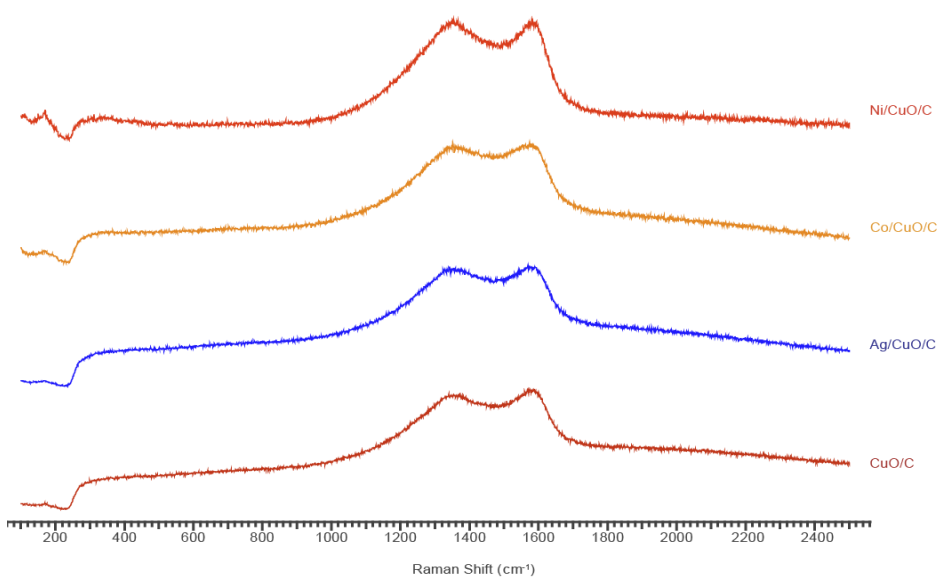


Figure S8. Raman spectra of the decomposition products after thermal initiation.

Table S2. XPS – CuO@C.

CuO@C	C 1s (33.09 wt%)					O 1s (16.26 wt%)		
	C=C sp ²	C-O	C-N	C=O	π-π*	Cu-O/OH	C-OH	C=O
At%	31.82	13.37	3.19	5.33	2.25	13.88	6.02	0.75
Wt%	18.81	7.90	1.89	3.15	1.33	10.93	4.74	0.59
BE	284	285.3	288.1	286.6	290.1	531.3	533	535.7

CuO@C	N 1s (6.36 wt%)			Cu 2p (44.29 wt%)					
	C-N-Cu	Gra(C)-N	Ox-N	Cu ^{0/+} (3/2)	Cu ²⁺ (3/2)	Cu ^{0/+} (1/2)	Cu ²⁺ (1/2)	Cu ^{0/+} (3/2 sat)	Cu ²⁺ (1/2 sat)
At%	6.39	1.12	1.71	2.62	2.24	2.59	2.22	2.53	1.96
Wt%	4.41	0.77	1.18	8.19	7.00	8.10	6.94	7.91	6.13
BE	398.7	400.7	405.8	932.5	934.4	952.1	954.4	~939	~962

Table S3. XPS – Ni-CuO@C.

Ni-CuO@C	C 1s (33.94 wt%)					O 1s (16.51 wt%)		
	C=C sp ²	C-O	C-N	C=O	π-π*	Cu-O/OH	C-OH	C=O
At%	31.69	12.48	3.33	5.23	2.67	12.35	6.72	1.16
Wt%	19.41	7.65	2.04	3.20	1.64	10.08	5.48	0.95
BE	284	285.4	288.1	286.7	290	531.1	532.6	535

Ni-CuO@C	N 1s (8.3 wt%)			Cu 2p (40.0 wt%)					
	C-N-Cu	Gra(C)-N	Ox-N	Cu ^{0/+} (3/2)	Cu ²⁺ (3/2)	Cu ^{0/+} (1/2)	Cu ²⁺ (1/2)	Cu ^{0/+} (3/2 sat)	Cu ²⁺ (1/2 sat)
At%	7.66	1.69	2.27	2.05	1.82	2.03	1.8	3.16	1.48
Wt%	5.47	1.21	1.62	6.65	5.90	6.58	5.83	10.24	4.80
BE	398.8	401.5	405.8	932.3	934.2	952.1	954.3	~940	~962

Ni-CuO@C	Ni 2p (1.26 wt%)	
	Ni ²⁺ (3/2)	Ni ²⁺ (1/2)
At%	0.21	0.21
Wt%	0.63	0.63
BE	854.8	872

Table S4. XPS – Co-CuO@C.

Co-CuO@C	C 1s (37.16 wt%)					O 1s (17.18 wt%)		
	C=C sp ²	C-O	C-N	C=O	π-π*	Cu-O/OH	C-OH	C=O
At%	30.9	14.6	4.49	6.45	2.5	11.78	6.9	1.78
Wt%	19.48	9.20	2.83	4.07	1.58	9.89	5.79	1.50
BE	284	285.5	288.7	287.1	291	531.3	532.9	535.4

Co-CuO@C	N 1s (6.52 wt%)			Cu 2p (39.13 wt%)					
	C-N-Cu	Gra(C)-N	Ox-N	Cu ^{0/+} (3/2)	Cu ²⁺ (3/2)	Cu ^{0/+} (1/2)	Cu ²⁺ (1/2)	Cu ^{0/+} (3/2 sat)	Cu ²⁺ (1/2 sat)
At%	6.43	1.02	1.42	1.79	1.76	1.78	1.74	3.33	1.33
Wt%	4.73	0.75	1.04	5.97	5.87	5.94	5.80	11.11	4.44
BE	398.8	401.5	405.5	932.3	934.1	952	954.2	~940	~962

Table S5. XPS – Ag-CuO@C.

Ag-CuO@C	C 1s (43.46 wt%)					O 1s (25.63 wt%)		
	C=C sp ²	C-O	C-N	C=O	π-π*	Cu-O/OH	C-OH	C=O
At%	26.3	21.79	5.96	7.32	0.07	14.99	11.75	0.46
Wt%	18.60	15.41	4.22	5.18	0.05	14.12	11.07	0.43
BE	284	285.1	288.4	286.4	291	531.6	533.1	535.4

Ag-CuO@C	N 1s (3.58 wt%)			Cu 2p (25.49 wt%)					
	C-N-Cu	Gra(C)-N	Ox-N	Cu ^{0/+} (3/2)	Cu ²⁺ (3/2)	Cu ^{0/+} (1/2)	Cu ²⁺ (1/2)	Cu ^{0/+} (3/2 sat)	Cu ²⁺ (1/2 sat)
At%	2.36	1.22	0.76	0.9	1.2	0.89	1.19	1.67	0.96
Wt%	1.95	1.01	0.63	3.37	4.49	3.33	4.45	6.25	3.59
BE	398.3	400.1	405.9	932.3	934.2	951.8	954.1	~940	~962

Ag-CuO@C	Ag 3d (1.84 wt%)	
	Ag ⁺ (5/2)	Ag ⁺ (3/2)
At%	0.15	0.14
Wt%	0.95	0.89
BE	367.1	373.8

Table S6. Metal loading wt% obtained from XPS.

Catalyst	Cu loading (wt%)	M loading (wt%)	Cu : M ratio	Total metal loading (wt%)
CuO@C	44.29	---	44.29	44.29
Ni-CuO@C	40.0	1.26	31.75	25.52
Co-CuO@C	39.13	---	39.13	39.13
Ag-CuO@C	25.49	1.84	13.85	27.33

6. Scanning Transmission Electron Microscopy-Energy Dispersive X-ray Spectroscopy

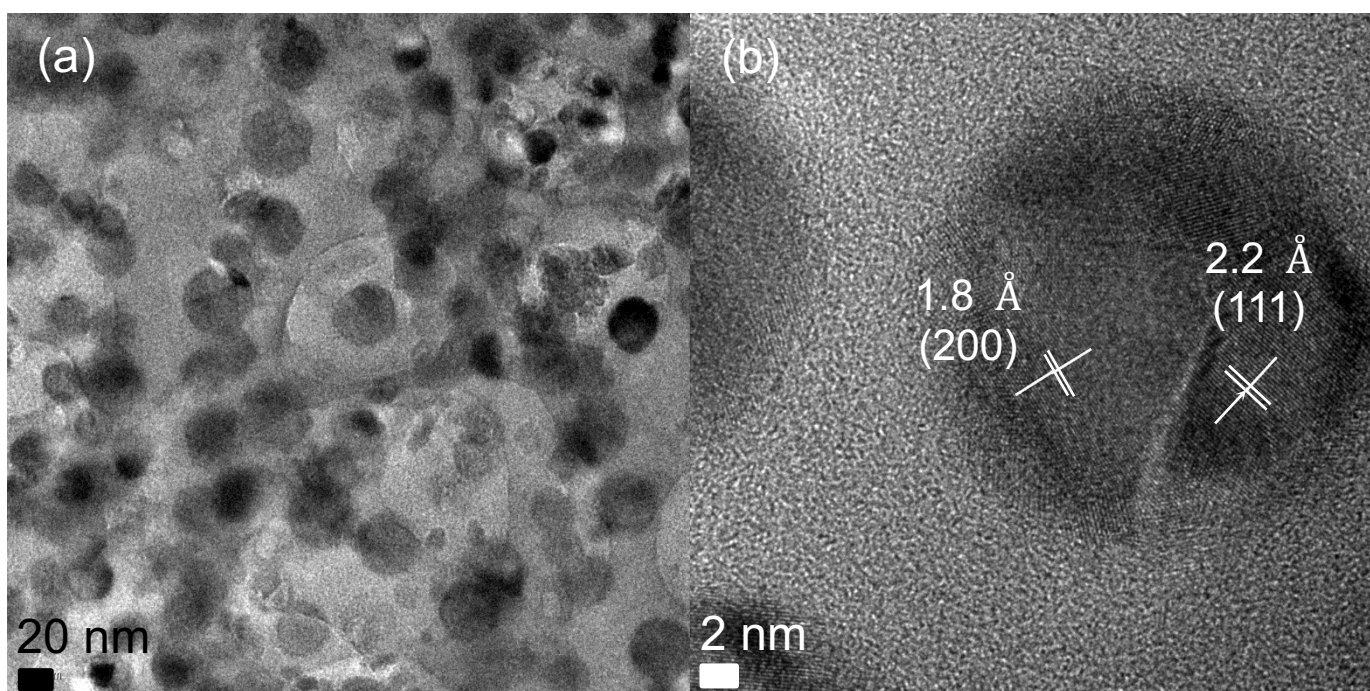


Figure S9 TEM images with analysis of lattice fringes for CuO@C.

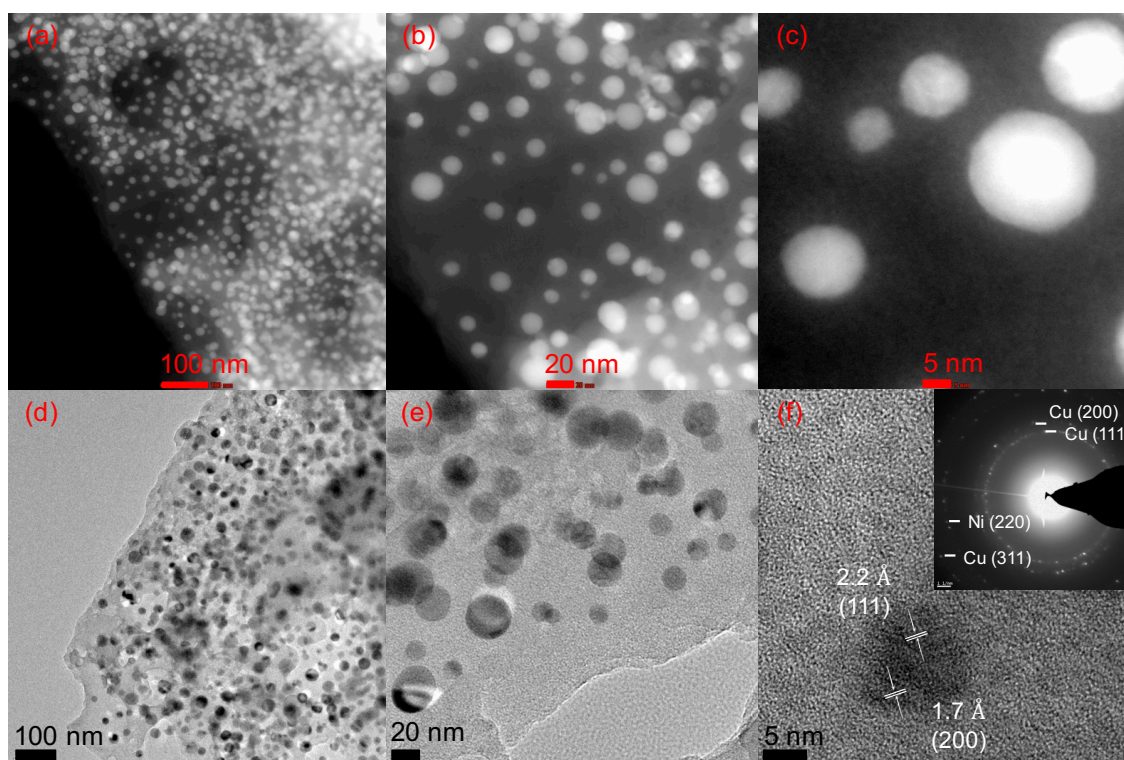


Figure S10 STEM images for Ni-CuO@C (dark field images) on top (a-c) and TEM images with analysis of lattice fringes and diffraction patterns inset (bright field images) on bottom (d-f).

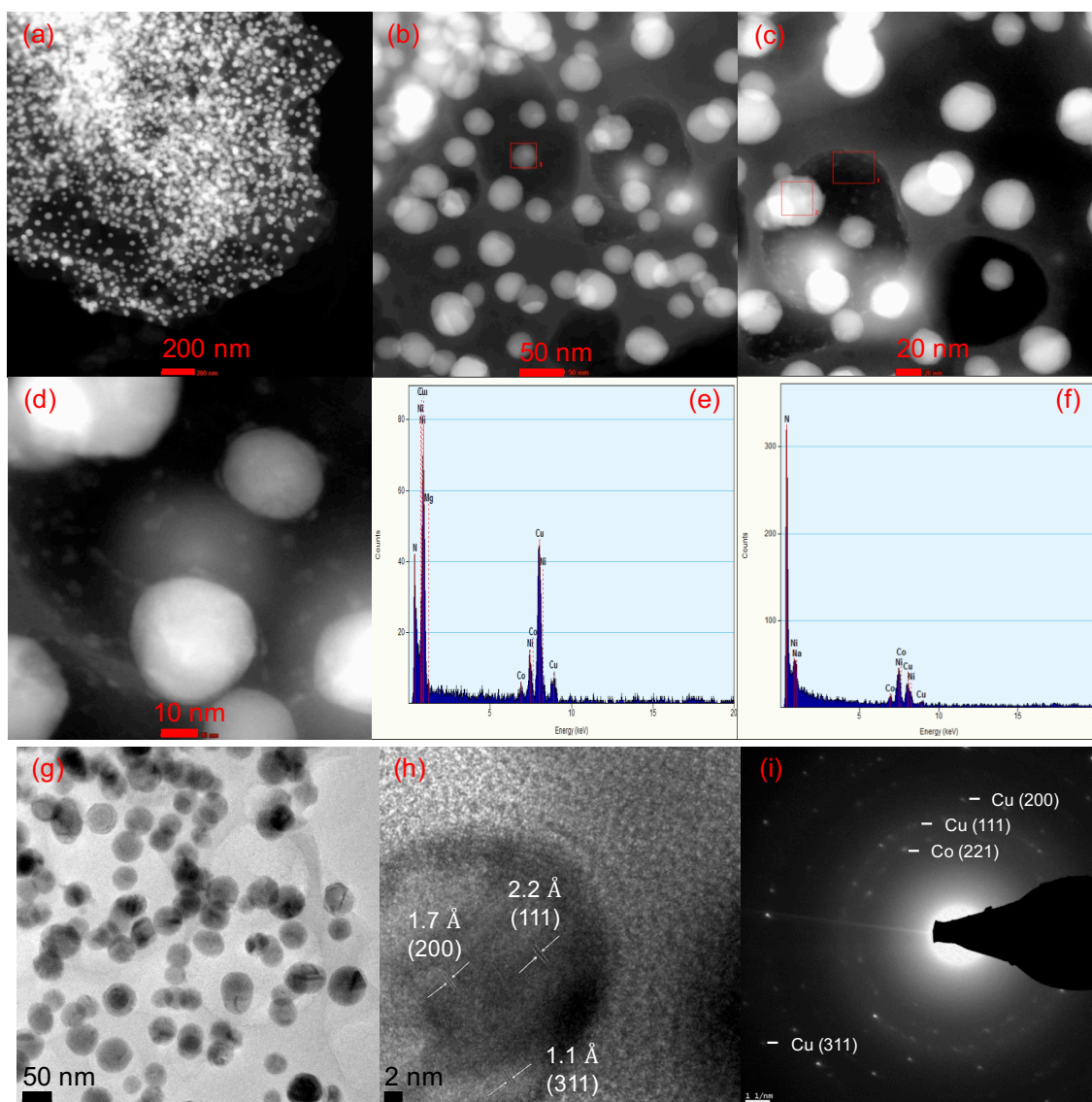


Figure S11. STEM images for Co-CuO@C (dark field images) with EDX analysis in selected particles and region on top (a-f), and TEM images with analysis of lattice fringes and diffraction patterns (bright field images) on bottom (h-i).

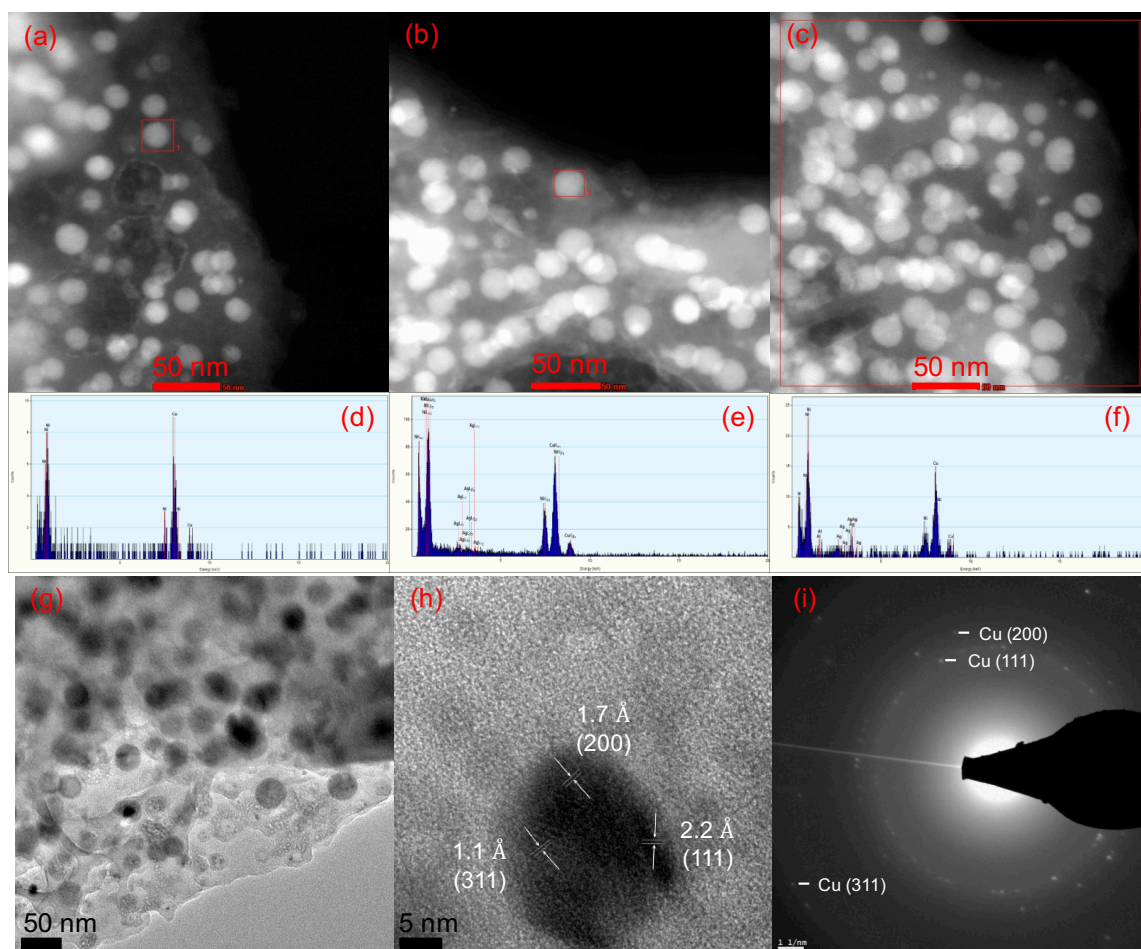


Figure S12. STEM images for Ag-CuO@C (dark field images) with EDX analysis in selected particles and region on top and TEM images with analysis of lattice fringes and diffraction patterns (bright field images) on bottom.

7. Reduction of 4-Nitrophenol Obtained from UV-Vis

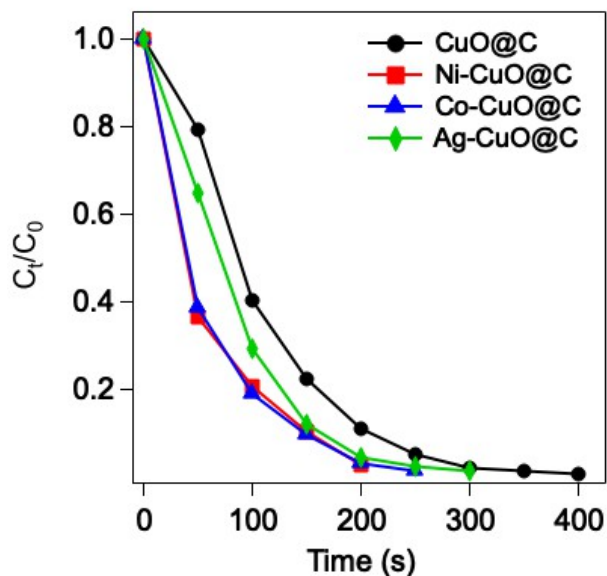


Figure S13. The plots of C_t/C_0 against reaction time.

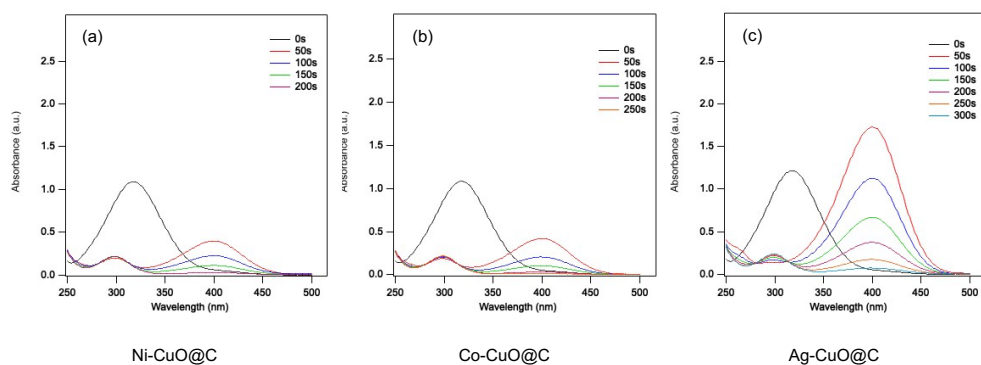


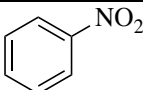
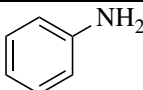
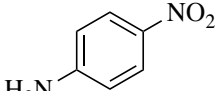
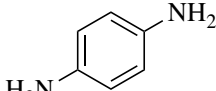
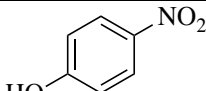
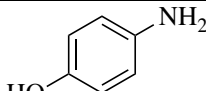
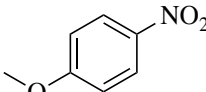
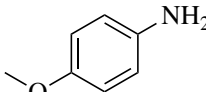
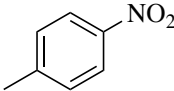
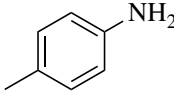
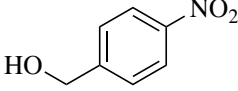
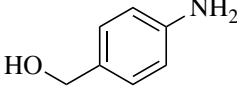
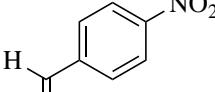
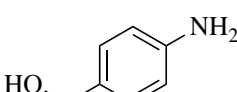
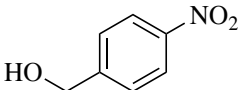
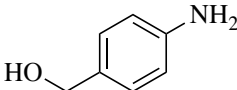
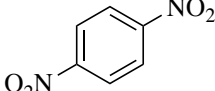
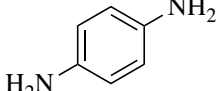
Figure S14. Time-dependent UV-Vis absorption spectra of the 4-nitrophenol reduced by NaBH_4 with Ni-CuO@C (a), Co-CuO@C (b), and Ag-CuO@C (c) at room temperature.

Table S7. Reaction rates of the catalytic reduction for 4-NP by CuO@C and M-CuO@C at different temperatures.

Temp. (K)	Rate Constant (min^{-1})			
	CuO@C	Ni-CuO@C	Co-CuO@C	Ag-CuO@C
288	0.342	1.224	0.738	0.45
296	0.804	1.578	1.056	0.876
300	1.062	1.818	1.278	1.218
303	1.398	1.956	1.404	1.566

8. Reduction of 4-Nitro-aromatic Compounds Obtained from UV-Vis

Table S8. Reduction of various nitroaromatic compounds by Ni-CuO@C in aqueous solution.

#	Substrate	Product	Time (min)	Rate constant, k (min ⁻¹)	Substituent constant, σ^2
1			9.2	0.18	0
2			14.2	0.183	-0.66
3			3.3	1.092	-0.37
4			12.5	0.138	-0.27
5			9.2	0.192	-0.17
6			10	0.177	0
7			10	0.189	0.42
8			0.83	1.515	0.45
9			13.3	0.174	0.79

^a All of the reactions were carried out according to the general experimental procedure at room temperature.

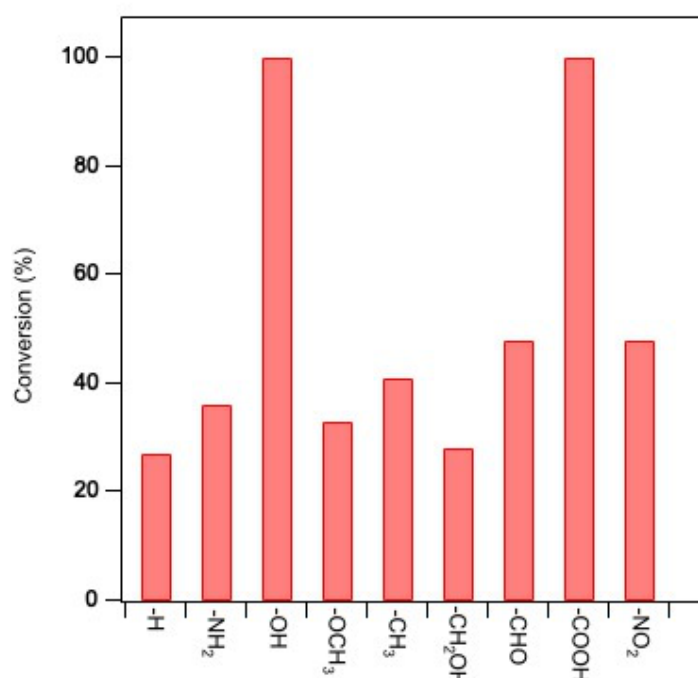


Figure S15. (a) The Ni-CuO@C catalyzed conversion efficiencies in the first 3 min of the reduction reaction for substituted nitrobenzenes at 25 °C.

Table S9 Comparison of catalytic activity for the reduction of 4-nitrophenol with the synthesized catalysts and the other reported catalysts.

Entry	Catalyst	Turnover rate (mmol/g _{cat} /min)	Rate constant <i>k</i> (min ⁻¹)	Activity factor <i>K</i> (min ⁻¹ ·g _{cat} ⁻¹)	Ref
1	CuO@C	6	0.804	804	this work
2	Ni-CuO@C	12	1.578	1578	this work
3	Co-CuO@C	9.6	1.06	1056	this work
4	Ag-CuO@C	8.0	0.88	876	this work
6	GO/Cu	0.17	5.04	229	56
7	Cu ₂ O/PEG-ZT	1.04	1.07	72	57
9	Cu/AC-600-1	0.06	0.78	782	58
10	Cu@CH + GO	0.01	0.91	182	59
11	RGO-CuNi	0.40	0.89	178	60
12	Co-Cu/CB-CS	0.003	0.64	43	61
13	Ag-Cu BNPs	0.002	0.18	18	62
14	Au/AC	0.001	0.25	127	63
15	Au/CuO	0.18	0.10	1280	36
16	PdNPs@Pct-CMC/Fe ₃ O ₄	0.01	0.67	125	64

^a All of the reactions were carried out according to the general experimental procedure at room temperature

9. References

¹ Feldblyum, J. I.; Liu, M.; Gidley, D. W.; Matzger, A. J., *J. Am. Chem. Soc.*, **2011**, *133*, 18257-18263.

² Hansch, C.; Leo, A.; Taft, R. W. A Survey of Hammett substituent constants and resonance and field parameters. *Chem. Rev.* **1991**, *91*, 165-195.